PCCP

Dynamic Article Links

901

PAPER

Quantification of photoelectrogenerated hydroxyl radical on TiO$_2$ by surface interrogation scanning electrochemical microscopy†

Dodzi Zigah, Joaquín Rodríguez-López and Allen J. Bard*

The surface interrogation mode of scanning electrochemical microscopy (SI-SECM) was used for the detection and quantification of adsorbed hydroxyl radical $^\bullet$OH$_{(ads)}$ generated photoelectrochemically at the surface of a nanostructured TiO$_2$ substrate electrode. In this transient technique, a SECM tip is used to generate *in situ* a titrant from a reversible redox pair that reacts with the adsorbed species at the substrate. This reaction produces an SECM feedback response from which the amount of adsorbate and its decay kinetics can be obtained. The redox pair IrCl$_6^{2-/3-}$ offered a reactive, selective and stable surface interrogation agent under the strongly oxidizing conditions of the photoelectrochemical cell. A typical $^\bullet$OH$_{(ads)}$ saturation coverage of 338 μC cm^{-2} was found in our nanostructured samples by its reduction with the electrogenerated IrCl$_6^{3-}$. The decay kinetics of $^\bullet$OH$_{(ads)}$ by dimerization to produce H$_2$O$_2$ were studied through the time dependence of the SI-SECM signal and the surface dimerization rate constant was found to be $\sim k_{OH} = 2.2 \times 10^3$ mol^{-1} m^2 s^{-1}. A radical scavenger, such as methanol, competitively consumes $^\bullet$OH$_{(ads)}$ and yields a shorter SI-SECM transient, where a pseudo-first order rate analysis at 2 M methanol yields a decay constant of $k'_{MeOH} \sim 1$ s^{-1}.

Introduction

One of the most studied semiconductor is TiO$_2$, indeed the anatase form of TiO$_2$ is a good semiconductor photocatalyst with a large band gap ($\sim$3.2 eV) and is widely used as the photoanode in biased water splitting electrolysis cells to produce O$_2$,[1–4] as well as in the photodegradation of organic pollutants.[5–8] These photoinduced reactions are thought to proceed through the $^\bullet$OH$_{(ads)}$ intermediate. When TiO$_2$ is illuminated, an electron (e$^-$) in the conduction band and a hole (h$^+$) in the valence band are generated, eqn (1). On the TiO$_2$ surface, $^\bullet$OH$_{(ads)}$ is formed as a consequence of the abstraction of an electron from water or hydroxyl ion by the electrogenerated hole as shown in eqn (2) for water in acidic media.[9–12] In an electrolytic cell, the promoted electron is conducted through the external circuit to the cathode.

$$\text{TiO}_2 + h\nu \rightarrow \text{e}^- + \text{h}^+ \tag{1}$$

$$\text{H}_2\text{O} + \text{h}^+ \rightarrow {}^\bullet\text{OH}_{(ads)} + \text{H}^+ \tag{2}$$
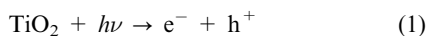
Here, photogenerated hydroxyl radical, $^\bullet$OH$_{(ads)}$, adsorbed on a nanostructured polycrystalline TiO$_2$ surface was studied

Center for Electrochemistry, Department of Chemistry and Biochemistry, University of Texas at Austin,
1 University Station A5300, Austin, Texas 78712-0165, USA.
E-mail: ajbard@mail.utexas.edu
† Electronic supplementary information (ESI) available: Photocurrent measurement and simulation results. See DOI: 10.1039/c2cp40907k

by scanning electrochemical microscopy in the surface interrogation mode (SI-SECM).[13,14] SI-SECM transients were used to quantify this species in the dark and to determine its decay kinetics by dimerization to H$_2$O$_2$ and by reaction with methanol, used as a model scavenger.

Understanding the reactivity of $^\bullet$OH$_{(ads)}$ is important for improving the photocatalytic activity of TiO$_2$ and of other materials.[15–18] SI-SECM has been recently introduced as an *in situ* technique for the detection and quantification of adsorbed intermediates in electrochemical systems. Vacuum techniques such as X-ray photoelectron spectroscopy (XPS) have been used widely to study $^\bullet$OH$_{(ads)}$ on TiO$_2$,[11,19–21] as well as spin trapping techniques,[22–24] but the direct quantification of this species in an electrolytic environment is desirable. In the present work we used SI-SECM, where a reversible redox mediator generated at an ultramicroelectrode (UME) tip is used to "micro-titrate" the photogenerated adsorbed species. SECM has been used previously in studies of semiconductor electrodes, *e.g.* in the etching of semiconductor surfaces[25] and the study photoelectron transfer (PET) kinetics at the semiconductor/electrolyte interface.[26] SI-SECM has been already employed successfully in the detection of electrogenerated oxide species on the surface of Au and Pt,[14,27] and H$_{(ads)}$[28] and CO$_{(ads)}$[29] on Pt. In this study, SI-SECM is introduced for the quantification and study of the reaction dynamics of intermediate species resulting from photoprocesses at a semiconducting material. Unlike noble metal surfaces, where certain adsorption features can be partially

identified and quantified by direct electrochemical techniques such as cyclic voltammetry (CV), the resulting voltammogram at a TiO$_2$ electrode provides little insight about the amounts of adsorbed species generated by the reaction in eqn (2). Furthermore, the interaction and decay of these species at open circuit cannot be followed by conventional electrochemical techniques. This is clearly of interest in understanding more complex reactions, *e.g.* pollutant remediation, where the interplay between $^\bullet$OH$_{(ads)}$ and other adsorbed intermediates through Langmuir–Hinshelwood mechanisms, or with species in solution through Eley–Rideal type mechanisms determines their efficiency. Moreover, an understanding of the product distribution is important in energy-related processes such as oxygen evolution (where electrolysis of water can yield O$_2$ or H$_2$O$_2$), and can be achieved through the time-resolved quantification of $^\bullet$OH$_{(ads)}$. In this study, we treat the case of the simplest $^\bullet$OH$_{(ads)}$ decay process through its dimerization to form H$_2$O$_2$ as shown in eqn (3), and we further elaborate another model process, the scavenging of $^\bullet$OH$_{(ads)}$ by aqueous methanol as shown in eqn (4). Here we prove the utility of SI-SECM to investigate processes at photoelectrocatalysts by using a proof-of-concept approach on nanostructured TiO$_2$ but expect that this strategy will be useful for other semiconductor photocatalyst structures, such as well-defined single crystal surfaces.

$$2^\bullet\text{OH}_{(ads)} \rightarrow \text{H}_2\text{O}_2 \quad k_{\text{OH}} \quad (3)$$

$$^\bullet\text{OH}_{(ads)} + \text{CH}_3\text{OH} \rightarrow \text{products} \quad k'_{\text{MeOH}} \quad (4)$$
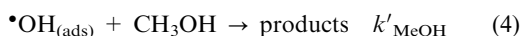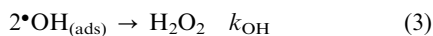
Mode of operation

The SI-SECM mode consists of a specific application of the feedback mode of SECM[13] under transient conditions, which allows for the quantification of finite amounts of adsorbed reactive species at a substrate. In SI-SECM, an SECM tip (an UME) is approached to a substrate electrode of the material of interest. This substrate generates an adsorbed intermediate on its surface and is then allowed to rest at open circuit. Following this, a reactive redox mediator generated at the SECM tip diffuses towards it and reacts chemically with the adsorbed intermediate. The tip current during this last stage reports the amount of adsorbate to the SECM tip through a transient feedback loop, that is, an increased current that lasts as long as adsorbate is present at the substrate. The magnitude and shape of the tip signal allows the quantification of the adsorbate[14] and to determine its reaction kinetics with respect to the mediator.[27]

It is desirable that the size of the active parts of the tip and substrate are of the same dimension and typically the SI-SECM analysis is carried out with UMEs with radius ≤20 μm. Larger electrodes can be employed as long as they are well aligned.[28] With conductive substrates the requirement that the substrate size be similar to that of the tip arises because of the existence of open circuit feedback at large unbiased electrodes,[30,31] which is minimized by this geometric constraint without sacrificing analytical performance. In the present study this issue was of less concern because of the semiconducting properties of the substrate, where the behavior of
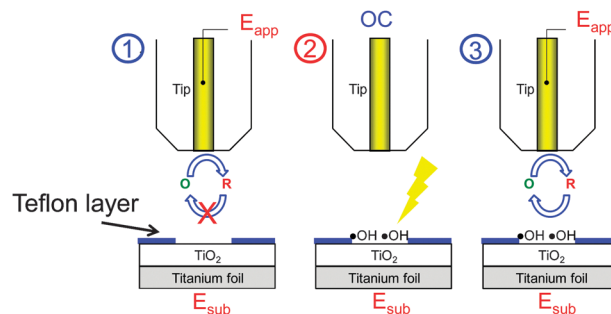
Scheme 1 Description of the surface interrogation technique for the reduction of $^\bullet$OH$_{(ads)}$ on TiO$_2$. (1) No $^\bullet$OH$_{(ads)}$ on TiO$_2$; the reduced species generated at the tip cannot react with the surface. (2) Tip is at open circuit and light is turned on; $^\bullet$OH$_{(ads)}$ are generated on TiO$_2$ through surface irradiation. (3) Light is turned off, interrogation of $^\bullet$OH$_{(ads)}$ takes place by reduced species generated at the tip.

TiO$_2$ in the dark is close to that of an insulator. This generates a negligible open circuit feedback background in the dark, so it is possible to have a larger active area of the substrate. It is still desirable to restrict its size, however, so that one can measure adsorbate coverage values with respect to a known area.

Scheme 1 describes the mode of operation of SI-SECM for the generation and the detection of $^\bullet$OH$_{(ads)}$ on the TiO$_2$ substrate. The substrate consists of a Teflon layer deposited over a large substrate of TiO$_2$ where a hole ($\sim$300 μm) is produced in this Teflon layer to expose a TiO$_2$ microelectrode.[32] The SI-SECM technique is divided in three steps as shown in Scheme 1. In the initial step, the tip is approached to the substrate. For a tip with radius $a = 50$ μm, the distance with respect to the substrate was typically set at $d \sim 25$ μm. A potential is then applied to the tip to produce a reduced mediator species Red at a diffusion limited rate from an oxidized species Ox initially present in the electrolyte. Provided no $^\bullet$OH$_{(ads)}$ is present on the substrate (*e.g.* in the dark) a negative feedback is observed. In the second step, TiO$_2$ is put under illumination and $^\bullet$OH$_{(ads)}$ is produced. During this time, the tip is turned off and allowed to rest at open circuit. In the third step, the TiO$_2$ substrate is returned to the dark, and the production of $^\bullet$OH$_{(ads)}$ ceases. After a time delay, a potential is applied to the tip to produce again Red which diffuses towards the substrate and reacts with $^\bullet$OH$_{(ads)}$ to give a transient positive feedback as a result of the regeneration of Ox as shown in eqn (5).

$$^\bullet\text{OH(ads)} + \text{Red} \rightarrow \text{OH}^- + \text{Ox} \quad k_{\text{SI}} \quad (5)$$

When all the adsorbate species have reacted with Red, negative feedback behavior is observed again and the substrate electrode returns to its initial state. Fig. 1 shows these steps on a typical feedback chronoamperogram.[33,34] In region 1 of Fig. 1, the tip is preconditioned to negative feedback in the absence of light and chemical reaction at the substrate. In region 2 the tip is disconnected from the setup and no tip signal is recorded; during this time the substrate is photo activated and generates $^\bullet$OH$_{(ads)}$. Finally in region 3, the system is brought back to dark conditions and the tip is activated and generates the reduced species Red at a diffusion limited rate. A transient positive feedback is observed if
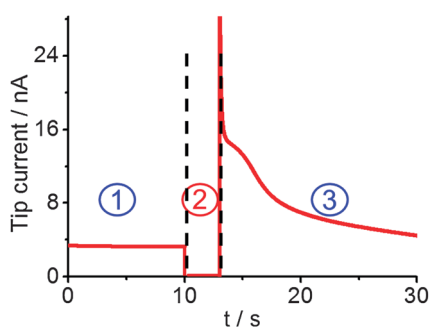
Fig. 1 Tip current as a function of time during the three steps described in Scheme 1. (1) Tip current displays negative feedback; (2) tip is at open circuit and substrate is irradiated; (3) light off, tip is activated.

Fig. 2 (━━) Photocurrent and (━━) dark current on TiO_2 in NaOH 1 M solution, under xenon lamp irradiation 100 mW cm^{-2}.

$^{\bullet}OH_{(ads)}$ is present at the substrate. In this SI-SECM experiment it is possible to apply a potential on the substrate during the surface interrogation process. Because TiO_2 is an n-type semiconductor, one can only oxidize electrochemically the reduced form of the mediator under illumination and negative feedback will be observed under any dark conditions in the absence of adsorbed $^{\bullet}OH_{(ads)}$. Note that in this study, we chose to use a front surface illumination of the semiconductor. An alternative setup to the one used here employs a deposited semiconductor on a transparent (e.g. ITO, FTO) substrate with back-illumination (through the FTO). This simplifies the illumination set-up and could still use insulation of the top surface with a Teflon layer as described below. However it cannot be used for semiconducting layers prepared from opaque substrates.

Experimental section

Chemicals

Deionized water (resistivity 18.2 MΩ) was used in all experiments. Chemicals were used as received: ammonium fluoride (98%), ferrocenemethanol (97%), polytetrafluoroethylene (PTFE 60 wt% dispersed in water), from Aldrich; perchloric acid (67–71%) trace metal, methanol, acetone, ethanol, ethylene glycol, sodium phosphate monobasic monohydrate (99.5%), phosphate dibasic anhydrous (99.9%), lead dioxide (97%), agar purified grade, sodium hydroxide (99.2%) from Fisher Scientific; potassium hexachloroiridate(III), $K_3Ir(III)Cl_6$, was synthesized in our group and used as starting material for the in situ preparation of the hexachloroiridate(IV) ion, $Ir(IV)Cl_6^{2-}$, in the electrochemical cell by passing it through PbO_2.

Electrodes

In all experiments a Ag/AgCl reference electrode (saturated KCl, 0.197 V vs. NHE) was used. In order to prevent chloride leakage from this reference, a 0.2 M sodium perchlorate 4% w/v agar salt bridge was used with the reference electrode. Gold (99.99%) from Goodfellow (Devon, PA), 1 mm diameter wire, was used during all the SI-SECM experiments as the counter electrode. Gold 100 μm diameter wire was used to make a tip microelectrode with an RG = 3 (RG = r_g/a where r_g is the radius of the flat end of the SECM tip including the sheath of glass surrounding the metal disk). The tip electrode was
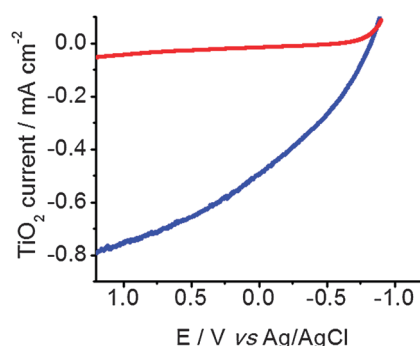
polished prior to use with the alumina paste (0.05 μm) on microcloth pads (Buehler, Lake Bluff, IL), and sonicated for 15 min in water. Electropolishing and cleaning of the tip was done by cycling between −0.5 and 1.7 V vs. Ag/AgCl in 1 M perchloric acid.

For the nanostructured TiO_2 substrate, titanium foil of 0.25 mm thickness (99.7%) from Aldrich was cut into squares of 2.25 cm^2, these pieces of titanium were cleaned successively in methanol, ethanol and water for 15 min by sonication. After the cleaning procedure TiO_2 was produced by electrochemical anodization. Briefly, the anodization was carried out in a home-made SECM cell in a two-electrode configuration where the counter electrode was a graphite rod. A power supply (Burleigh) was used to apply 60 V during 6 h to the electrodes in a solution of ethylene glycol with 0.25 wt% NH_4F and 1% H_2O. The morphology of the resulting electrodes has been discussed in detail previously.[35] SEM pictures of typical samples are shown in Fig. S1 (ESI†).

After anodization, the TiO_2 was annealed at 625 °C for 1 h in ambient atmosphere (heating rate of 1 °C min^{-1}) and was then allowed to cool back to ambient conditions. TiO_2 substrates were tested in 1 M NaOH and checked to provide at least a photocurrent of ∼0.8 mA cm^{-2} under a light irradiance of 100 mW cm^{-2} at 0.9 V vs. Ag/AgCl as shown in Fig. 2. The nanostructured TiO_2 electrodes used here have a thickness of ∼10 μm and a geometrical roughness factor of ∼500 according to dye desorption methods where typical coverage values are Γ_{dye} ∼ 60 × 10^{-5} mol m^{-2}, or a charge equivalent of ∼6 mC cm^{-2} assuming a 1e$^-$ conversion factor.[35] In order to obtain a quantitative approximation to our system, we modeled the SI-SECM response using commercial finite element method software, where we have considered our photocatalyst, i.e. ∼10 μm thick TiO_2, as a continuous medium where the reactive mediator can access its surface homogeneously to provide feedback at the SECM tip. The model is described in the ESI.†

To complete the preparation of a micro-sized TiO_2 surface necessary to confine the surface, an insulating Teflon layer was selectively deposited using a previously reported technique.[32] The TiO_2 microelectrodes obtained had a diameter of 300 μm.

SI-SECM measurements

Measurements were performed using a CHI 900B (CH Instruments, Austin, TX) SECM bipotentiostat. A 150-W xenon

12766 | *Phys. Chem. Chem. Phys.*, 2012, **14**, 12764–12772

This journal is © the Owner Societies 2012

lamp (Oriel instrument, Newport corporation) was used to illuminate the TiO$_2$ surface as shown in Scheme 2. Before SI-SECM can be implemented, the tip and substrate must be concentrically aligned and approached to a μm distance. This was accomplished using the feedback mode, where a reversible redox mediator such as ferrocenemethanol (1 mM in 0.1 M pH = 7 phosphate buffer) is oxidized at the tip while the substrate is set at a potential where diffusion limited collection of the oxidized species is possible. Once the tip was aligned and positioned at a chosen height, the cell was thoroughly rinsed with deionized water and the interrogator mediator solution introduced into the cell. The tip-substrate alignment could not be accomplished through a substrate generation – tip collection scheme under illumination, since the movement of the tip above the substrate causes changes in the photon flux, which render the current–distance relationship untrustworthy. Furthermore, generation-collection strategies that included the tip collection of substrate generated oxygen (e.g. from water oxidation at TiO$_2$) often led to the undesirable formation of bubbles at the substrate. We found experimentally that, in the case of the collection of substrate-generated oxygen from water oxidation under illumination, the optimum distance, i.e. where the largest oxygen collection at the tip was observed, corresponded roughly to 25 μm.

SI-SECM was carried out in the chronoamperometry mode with a tip-substrate distance of ∼27 μm. The starting form of the mediator in the bulk solution was IrCl$_6^{2-}$ (Ox) from which IrCl$_6^{3-}$ (Red) was produced. The applied potential at the tip was chosen to ensure diffusion-limited conditions for the production of IrCl$_6^{3-}$ ($E_T = E_{reduction} = 0.7$ V vs. Ag/AgCl). For the generation of •OH$_{(ads)}$ under illumination, a potential $E_S = E_{oxidation}$ was chosen to be close to the current limited by the flux of photons, e.g. $E_S = 0.5$ V vs. Ag/AgCl (Fig. 2 and Fig. S2, ESI†). As depicted in Fig. 1, a typical SI-SECM measurement consisted of three steps: (1) preconditioning of the system in the dark ($E_T = 0.7$ V vs. Ag/AgCl, $E_S = 0.5$ V vs. Ag/AgCl); (2) generation of •OH$_{(ads)}$ under illumination for

a time τ_1 (tip at open circuit, $E_S = 0.5$ V vs. Ag/AgCl), and decay of adsorbed species for a time τ_2 in the dark (tip at open circuit, $E_S = 0.5$ V vs. Ag/AgCl); and (3) interrogation of adsorbed species in the dark ($E_T = 0.7$ V vs. Ag/AgCl, $E_S = 0.5$ V vs. Ag/AgCl) for 40 s.

Results and discussion

Choice of an interrogation mediator

The redox pair IrCl$_6^{2-/3-}$ at a concentration of 0.5 mM in 0.1 M HClO$_4$ was used as the mediator for interrogation of •OH$_{(ads)}$. This mediator has the following desirable properties: stability in the electrolyte, chemical reversibility, high solubility, reactivity with respect to the adsorbed species (i.e. is allowed thermodynamically and is fast) and low interaction with the substrate (e.g. provides low negative feedback in the absence of adsorbate).[27,29] •OH$_{(ads)}$ is a highly oxidizing intermediate with a standard potential of 1.9 V vs. NHE[36] and in principle a variety of reducible intermediates could be used to titrate it. In this study however, the stability requirement was crucial, because the intense UV light source in combination with the TiO$_2$ substrate provide a highly oxidizing environment. The IrCl$_6^{2-/3-}$ pair was found to satisfy this requirement. The use of its precursor potassium salt was also advantageous since no oxidizable counter-ions were present in solution. A final quality of the IrCl$_6^{2-/3-}$ pair was that its electrochemistry at the Au tip occurred at potential where collection of homogeneous substrate-generated products at pH = 1, i.e. H$_2$O$_2$ and O$_2$, did not interfere.

Shown in Fig. 3(A) is the cyclic voltammetry for the oxidation of the precursor IrCl$_6^{3-}$ and for the reduction of IrCl$_6^{2-}$ generated after chemical reaction of IrCl$_6^{3-}$ with the solid oxidizer PbO$_2$. The redox couple shows reversible behavior with $E_{1/2} = 0.85$ V vs. Ag/AgCl and is chemically stable during the experimental session. Furthermore, departure from this cyclic voltammetry (CV) behavior is not observed in the presence of oxygen (e.g. air saturation) or hydrogen peroxide (e.g. at 10 mM) in the solution. This indicates that the reduced form of the mediator does not react with species released into the microgap between the tip and the substrate and only reacts with species adsorbed at the substrate. A suitable tip potential, E_T, required for chronoamperometry under diffusion-limited conditions in the SECM setup was $E_T = 0.7$ V vs. Ag/AgCl. At this tip potential, the Au microdisk itself also does not detect species released into the microgap by the substrate. Fig. 3(B) shows a linear potential scan at the tip when the substrate is held at $E_S = 0.5$ V vs. Ag/AgCl under illumination in a solution that contains only HClO$_4$ (i.e. no mediator). In this case, the tip operates in the substrate generation – tip collection mode of SECM. Positive of $E_T = 0.4$ V vs. Ag/AgCl, no significant photogenerated products (O$_2$, H$_2$O$_2$) are detected at the Au microelectrode (a negligible background probably due to surface oxidation is only observed); these species are only sensed by the tip at potentials more negative than $E_T = 0.4$ V as evidenced in Fig. 3B. Thus, this ensures that the chronoamperometric changes in the signal at the tip in the SI-SECM experiment are only caused by the transient reaction of the reduced mediator with the adsorbed •OH$_{(ads)}$ at the substrate.
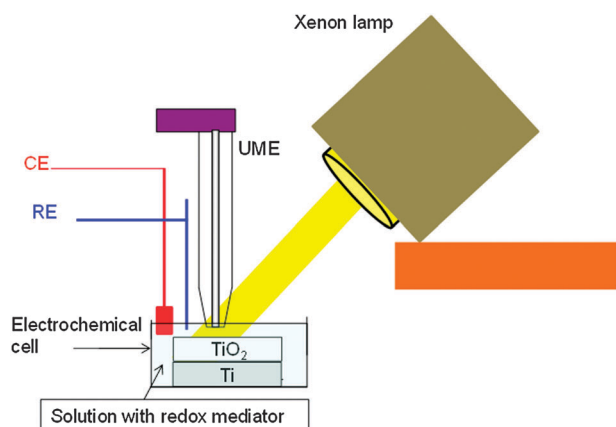
Scheme 2 Setup used for surface interrogation. The electrochemical cell was homemade and used a PTFE-selectively insulated Ti/TiO$_2$ plate as working electrode, Au SECM tip, Au counter electrode and a Ag/AgCl reference electrode with a NaClO$_4$ salt bridge. The cell contains a maximum of 1 mL of solution. A xenon lamp (100 mW cm^{-2}) was used (**Caution**: UV-absorbing glasses should be used for personal protection to avoid eye damage).
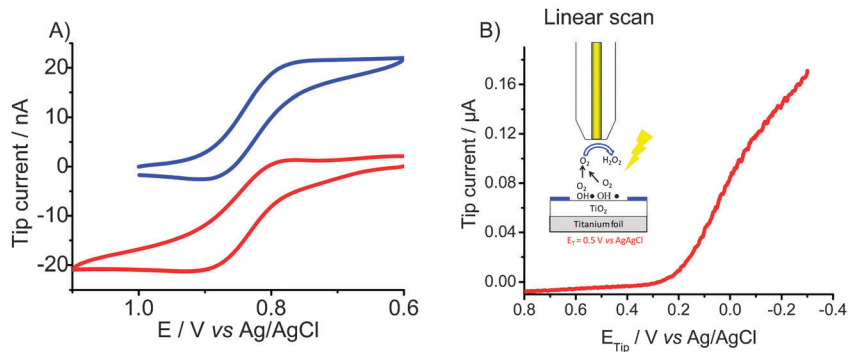
Fig. 3 (A) Cyclic voltammetry in 0.1 M HClO$_4$, scan rate 0.1 V s^{-1} of (—) K$_3$Ir^{III}Cl$_6$ and (—) K$_2$Ir^{IV}Cl$_6$ at 1 mM. (B) Substrate generation – tip collection on a Au tip. Linear scan at the tip, E_S = 0.5 V, light ON, 0.1 M HClO$_4$, scan rate = 0.1 V s^{-1}. O$_2$ is only detected at the tip at potentials more negative than E_T = 0.4 V.
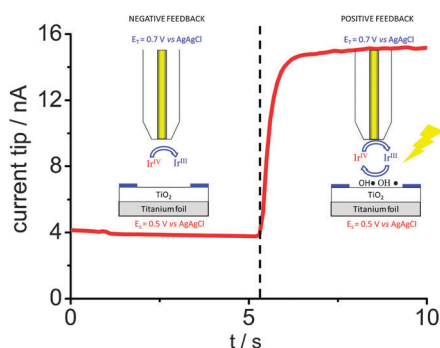
Fig. 4 Negative feedback in dark 0 s < t < 5 s; positive feedback under illumination 5 s < t < 10 s. Gold UME a = 50 μm, solution 0.1 M HClO$_4$, 0.5 mM K$_2$Ir^{IV}Cl$_6$, $d_{tip-sub}$ = 27 μm.

Preliminary SECM experiments were conducted to assure that negative feedback is observed under dark conditions while positive feedback is present only under or after illumination. Fig. 4 shows the evolution of the tip current (E_T = 0.7 V vs. Ag/AgCl, which at $d_{tip-sub}$ ~ 1000 μm displays a current $i_{T,inf}$ = 7 nA) as a function of the presence or absence of illumination at the substrate (E_S = 0.5 V vs. Ag/AgCl) when the interelectrode distance was ~27 μm (as measured from the bottom of the Ti plate to the tip). During the first five seconds, with the substrate in the dark, a negative feedback current is observed at the tip ($i_{T,NF}/i_{T,inf}$ = 0.57 compared to the predicted value, 0.56, at this value of $d_{tip-sub}$). For the following five seconds, the surface was illuminated and the current increased showing positive feedback ($i_{T,PF}/i_{T,inf}$ = 2.1 compared to a predicted value of ~2).[13] This value obtained for positive feedback suggests that temperature effects are not relevant in our setup, e.g. heating up of the solution would lead to higher mediator diffusion coefficients that would be reflected in a significantly larger positive feedback than predicted by theory.

Hydroxyl radical quantification

We assume that the reactive species at the substrate electrode is •OH$_{(ads)}$. The SI-SECM response at the interelectrode distance $d_{tip-sub}$ = 27 μm used is affected in absolute terms by the collection efficiency (CE) of the tip, where 0 < CE < 100%.[37] In the SI-SECM context, this parameter represents the ratio of

tip-recovered oxidized mediator produced at the substrate as a consequence of chemical reaction, a depiction of this process is shown in Fig. 5. In previous SI-SECM studies the ratio a/b, where a is the radius of the tip microdisk and b is that of the substrate respectively, has been larger or equal to 1 when the interelectrode distances were smaller than L = 0.2 (where L = $d_{tip-sub}/a$).[14,28,29] Under those conditions, CE is close to 100% and no correction is necessary.[14] When the ratio a/b < 1 and L > 0.2, as is the case of the present study, the absolute amount of adsorbed species can be obtained by incorporating CE through digital simulations,[27] as described in the following sections. For the present discussion, it is only necessary to keep in mind that CE is a geometrical factor that can be assumed to be constant provided the experimental setup and geometry is maintained for a set of experiments. We then present our initial results in terms of relative quantities from which qualitative trends can be deduced, to then arrive at the total simulated response of the system.

Fig. 6 shows an example of the experimental chrono-amperometric SI-SECM response to illustrate the method used for determining the relative charge equivalent •OH$_{(ads)}$ coverage. First a blank curve was recorded when no species are adsorbed on the substrate, as shown in Fig. 6(A) black curve, where a microelectrode Cottrell behavior is observed.

$$substrate: \cdot OH_{(ads)} + R \rightarrow OH^- + O$$
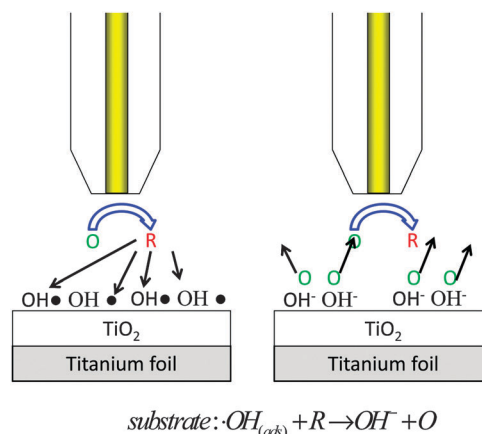
Fig. 5 Interrogation of TiO$_2$ by a reduced species. Due to geometric constraints, only a part of the oxidized species produced at the substrate can be fed back to the tip.

12768 | Phys. Chem. Chem. Phys., 2012, **14**, 12764–12772

This journal is © the Owner Societies 2012
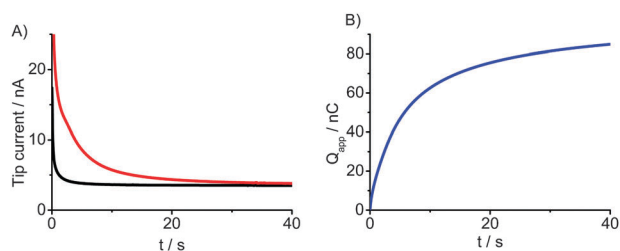
Fig. 6 (A) Experimental chronoamperometric curves for negative feedback (*e.g.* blank) (■) and for surface interrogation of $^\bullet OH_{(ads)}$ (■). TiO$_2$ microelectrode with radius $b = 150$ μm, interrogator: gold UME $a = 50$ μm; solution 0.1 M HClO$_4$ with 0.5 mM K$_2$Ir^{IV}Cl$_6$; $d_{tip-sub} = 30$ μm, illumination time τ_1 for $^\bullet OH_{(ads)}$ generation was 5 s and $E_S = 0.5$ V *vs.* Ag/AgCl. (B) Integrated charge for interrogation curve in (A) (■).

After the substrate is illuminated and hydroxyl radical is generated, the interrogation curve shows transient positive feedback. Fig. 6(A) (red curve), exhibits a higher current than the negative feedback blank. This increased current is the result of the reaction between $^\bullet OH_{(ads)}$ and the reduced form of the mediator. The transient positive feedback decreases with time and tends to reach the current obtained under negative feedback conditions, indicating consumption of the adsorbate. The tip creates a diffusion layer in the interelectrode gap, which titrates preferentially the area directly below it.[33,34] Subtraction of the SI-SECM transient from the blank yields the current due to the chemical reaction of the mediator with the adsorbate. The integrated value yields the amount of equivalent charge titrated, Fig. 6(B). With this charge we can calculate the "apparent" surface concentration for the hydroxyl radical on TiO$_2$:

$$\Gamma_{app} = \frac{Q_{app}}{nFA_{proj}} \qquad (6)$$

Where Q_{app} is the apparent charge that we obtain by the current integration and equivalent to $Q \times CE$ where Q is the actual charge equivalent titrated, *i.e.* from all surface species reacted regardless of the measurement geometry, n is the number of electrons exchanged in the chemical reaction and equal to 1, F is the Faraday's constant and A_{proj} is an approximation to the projected area titrated by the tip.

The described method can be first used to determine the time τ_1 required to attain limiting $^\bullet OH_{(ads)}$ coverage at the TiO$_2$ surface when no delay time τ_2 is chosen between the end of the illumination period and the interrogation process. This is shown in Fig. 7, where τ_1 is sampled between 0.1 s and 5 s; a limiting coverage is obtained at $\tau_1 > 2$ s under these conditions and this value is used to normalize the response. For the study of the open circuit decay of $^\bullet OH_{(ads)}$ a constant value of $\tau_1 = 3$ s was used, a suitable time to saturate the surface but short enough to prevent the evolution of bubbles from the substrate. For the maximum surface concentration, we approached the CE value using the empirical expressions for this parameter with RG = 3 and $d/(a/b) = 91$ μm as suggested for SECM systems with dissimilar tip and substrate sizes at different interelectrode separations and RG.[37] Using eqn (6) and estimating the projected area as that of the substrate (*e.g.* making use of the fact that $r_{sub} = r_g$ in our system),
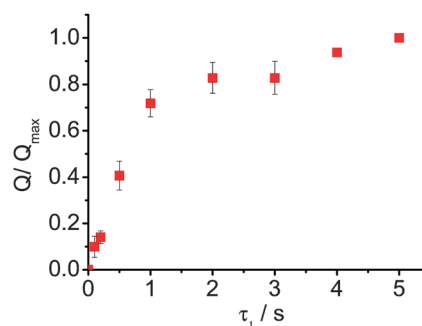
Fig. 7 $Q_{app}/Q_{app,max} = f(\tau_1)$, normalized charge for surface interrogation as a function of the illumination time.

we obtained CE = 0.44, then $Q = Q_{app}/CE$ predicts that the maximum surface concentration is 294 μC cm^{-2} in terms of charge or $\Gamma_{max} = 3.06 \times 10^{-5}$ mol m^{-2} in terms of amount of adsorbate.

Hydroxyl radical decay in dark

We studied the decay of $^\bullet OH_{(ads)}$ to form H$_2$O$_2$ at the TiO$_2$ surface due to its dimerization reaction (eqn (3)) as a function of the delay time between generation of the adsorbed $^\bullet OH$ and the surface interrogation, *i.e.* τ_2. This delay is depicted in Scheme 1 between the end of step 2 and the beginning of step 3. The quantified charge changes with respect to delay time, τ_2, as shown in Fig. 8(A). $^\bullet OH_{(ads)}$ is consumed by the dimerization reaction and there is a decrease in Q_{app} with increasing τ_2. The produced H$_2$O$_2$ does not react with the mediator and therefore SI-SECM is selective only towards the adsorbed species. For this second order kinetic process, a plot of $1/Q_{app}$ *vs.* τ_2 should yield a linear relationship, since Q_{app} is directly related to the surface coverage Γ_{app} (eqn (6)). Such a plot is shown in Fig. 8(B) where there is acceptable agreement to the linear model with a correlation coefficient $R^2 = 0.99$, whereas if the decay is modeled as a first order process, *i.e.* spontaneous desorption of $^\bullet OH_{(ads)}$, the linear plot of $\ln(Q_{app})$ *vs.* τ_2 yields a correlation coefficient $R^2 = 0.94$. This strongly suggests that $^\bullet OH_{(ads)}$ is consumed through a second order process to generate H$_2$O$_2$. Note that in this first approximation, the obtained value is importantly convoluted with the time required to carry the SI-SECM analysis, and therefore one must turn to the simulation of the system to correct for this, as discussed in the following section.

Corrected surface concentration and rate constant for second order decay of $^\bullet OH_{(ads)}$ at TiO$_2$

The use of finite element simulations has allowed us previously to obtain high quality information about the SI-SECM process, *e.g.*, in the quantification of electrogenerated oxides on Pt and Au[14] and the determination of reaction constants between different mediators and Pt oxides.[27] Other finite element simulations have been applied to transient feedback SECM for non-electroactive substrates, where information about the 2D diffusion,[38] lateral charge transport[39,40] and adsorption/desorption[41] kinetics of adsorbates have been obtained through curve fitting, in our case we perform a quasi 2D simulation.
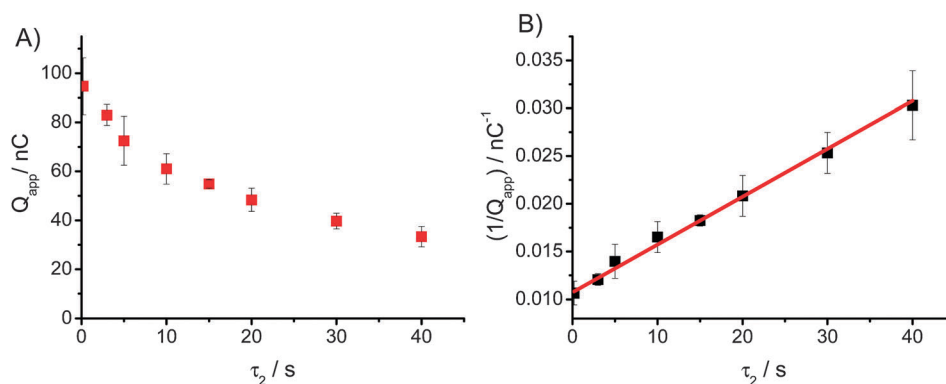
Fig. 8 (A) Apparent charge as function of the delay time $Q_{app} = f(\tau_2)$; (B) $1/Q_{app} = f(\tau_2)$. Slope = 5.0×10^{-4} nC^{-1} s^{-1}; intercept = 1.1×10^{-2} nC^{-1}; $r^2 = 0.99$.

Fig. 9 shows the fitting of simulated chronoamperograms to the experimental curves for the interrogation of $^\bullet$OH$_{(ads)}$ at TiO$_2$ with different delay times, τ_2, while Fig. 10 shows a comparison of the experimental curves of Fig. 9 at short interrogation times. To simplify the fitting of the curves through an initial value, we used the estimated maximum surface concentration of $^\bullet$OH$_{(ads)}$ found previously, i.e. $\Gamma_{max} = 3.06 \times 10^{-5}$ mol m^{-2}. The best fit was observed with $\Gamma_{max} = 3.5 \times 10^{-5}$ mol m^{-2} or 338 µC cm^{-2}. The surface coverage obtained in our samples was larger than the one observed for well-documented small species on smooth polycrystalline surfaces, e.g. for H$_{(ads)}$ on Pt the adsorbed charge is $Q_{(ads)} = 210$ µC cm^{-2}. The value obtained reflects the large surface area of the nanostructured morphology we used. Note however, that the charge value obtained is approximately 1/20 of the surface area determined for this type of sample from dye adsorption measurements, i.e. ~ 6 mC cm^{-2}, and thus indicates a much smaller coverage per active site than in the case of hydrogen on Pt. The present methodology can be used as a means of estimating the surface area in similar
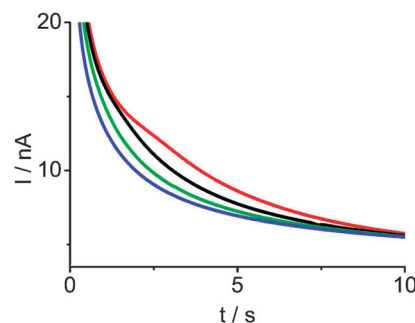
Fig. 10 Overlaid comparison of experimental curves for different delay times. (━━) $\tau_2 = 0.5$ s; (━━) $\tau_2 = 5$ s; (━━) $\tau_2 = 15$ s; (━━) $\tau_2 = 30$ s. All conditions as in Fig. 9.

high-roughness systems but also represents a first step to the determination of coverage parameters on better defined surfaces such as single crystal photoelectrocatalysts. SI-SECM has been shown to present a detection limit close to 2% of a monolayer of chemisorbed oxygen on smooth metal electrodes which makes it an appealing technique for studying surface dynamics.[14]

From the estimated value of Γ_{max} and the linearized relationship shown in Fig. 8(B), we can provide an initial guess for the second order decay constant, in this case, $k_{OH} = 1.5 \times 10^3$ mol^{-1} m^2 s^{-1}. The best fit value, which considers the impact of the delay time τ_2 on the measurement, the presence of decay during the interrogation time and the corrected value for Γ_{max} yielded $k_{OH} = 2.2 \times 10^3$ mol^{-1} m^2 s^{-1}. This value assumes that the formation of H$_2$O$_2$ resulting from the process shown in eqn (3) is the main channel for the decay of $^\bullet$OH$_{(ads)}$ under the open circuit conditions used, in the dark and in a timeframe where reasonably only $^\bullet$OH$_{(ads)}$, in contrast to reactive species such as "naked holes", are present ($t > 0.01$ ms). Another model parameter, (the rate constant for the SI process, k_{SI} was found to have the value $k_{SI} = 3$ m^3 mol^{-1} s^{-1}. Typical values for k_{SI} for interrogation of surface oxides on metallic electrodes are in the range 1 to 100 m^3 mol^{-1} s^{-1}. The value obtained is consistent with this range and is sufficient for quantitative work to be carried out.[27]

Methanol as a hydroxyl radical scavenger

Methanol is a good scavenger for hydroxyl radical,[42] and is often used as a sacrificial electron donor in photoelectrochemical
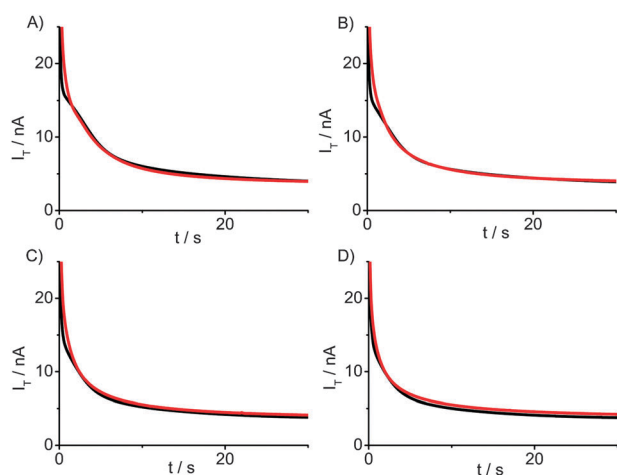
Fig. 9 Surface interrogation of $^\bullet$OH$_{(ads)}$ at different delay times, τ_2: (━━) experimental curve; (━━) theoretical curve. TiO$_2$ microelectrode with radius $b = 150$ µm, interrogator: gold UME $a = 50$ µm; solution 0.1 M HClO$_4$ with 0.5 mM K$_2$Ir^{IV}Cl$_6$; $d_{tip-sub} = 27$ µm, illumination time τ_1 for $^\bullet$OH$_{(ads)}$ interrogation was 3 s and $E_S = 0.5$ V vs. Ag/AgCl with (A) $\tau_2 = 0.5$ s, (B) $\tau_2 = 5$ s, (C) $\tau_2 = 15$ s, (D) $\tau_2 = 30$ s.

12770 | *Phys. Chem. Chem. Phys.*, 2012, **14**, 12764–12772

This journal is © the Owner Societies 2012
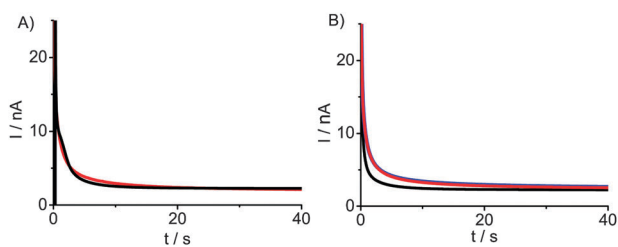
Fig. 11 TiO_2 microelectrode with radius $b = 150$ μm, interrogator: gold UME $a = 50$ μm; solution 0.1 M $HClO_4$ with 0.5 mM $K_2Ir^{IV}Cl_6$. $^\bullet OH_{(ads)}$ interrogation in the presence of methanol 2 M. $d_{\text{tip-sub}} = 25$ μm. (A) (━━) experimental curve delay time $\tau_2 = 0.3$ s; (━━) simulated curve; simulated with $\Gamma = 3.37 \times 10^{-5}$ mol m^{-2} and $k'_{\text{MeOH}} = 1$ s^{-1}; other parameters as described in text; (B) (━━) delay time $\tau_2 = 15$ s, (━━) $\tau_2 = 60$ s (━━) simulated curve for an insulating surface.

experiments producing formaldehyde in the reaction.[43] We explored the kinetics of this reaction, as shown in eqn (4), and carried out the interrogation process in the presence of an excess of methanol (2 M) so the reaction with $^\bullet OH_{(ads)}$ will be pseudo first-order. This reaction now occurs in parallel with the dimerization to H_2O_2, so the surface concentration of $^\bullet OH_{(ads)}$ should decay faster than shown in Fig. 10 for different values of τ_2. From the fit between experimental and theoretical curves we determined a value for this pseudo first-order rate constant of $k'_{\text{MeOH}} = 1$ s^{-1} for a short waiting time (0.3 s) Fig. 11A. This reaction is so fast that, for $\tau_2 > 5$ s, the interrogation curves resemble the insulating case, as shown in Fig. 11B. However, a complete fit to the complete negative feedback case was not achieved even at long τ_2. Possibly the reaction of methanol with hydroxyl radical leaves a intermediate at the TiO_2 surface (*e.g.* formaldehyde or its fragments)[44] that can also react with $^\bullet OH_{(ads)}$. We have previously reported the detection of reaction intermediates from the open circuit catalytic decomposition of formic acid at platinum by SI-SECM.[28] In that case, the Pt surface generated the detected species at open circuit. Here, activation of the electrode, possibly through the intermediacy of $^\bullet OH_{(ads)}$, is required to observe the discrepancy shown in Fig. 11(B). If the electrode is not photoactivated, the resulting curve follows well the simulated negative feedback response. Following similar arguments to those for $^\bullet OH_{(ads)}$, we found the limiting coverage of this adsorbed product to be $\Gamma_{\text{max}} = 0.70 \times 10^{-5}$ mol m^{-2} (or 67 μC cm^{-2}), which represents 1/5 of the maximum observed $^\bullet OH_{(ads)}$ in the absence of scavenger.

Methanol can react with hydroxyl radical and give a new species such as $^\bullet CH_2OH_{(ads)}$, eqn (7). This species can react with the mediator (eqn (8)), but $^\bullet CH_2OH_{(ads)}$ is also proposed to be further oxidized by O_2 (eqn (9)) produced during the photooxidation process to give HCHO and another product P.[43]

$$^\bullet OH_{(ads)} + CH_3OH \rightarrow {}^\bullet CH_2OH_{(ads)} + H_2O \quad k_{16} \quad (7)$$

$$^\bullet CH_2OH_{(ads)} + R \rightarrow {}^\bullet CH_2OH^- + O \quad k_{17} \quad (8)$$

$$^\bullet CH_2OH_{(ads)} + O_2 \rightarrow HCHO + P \quad k_{18} \quad (9)$$
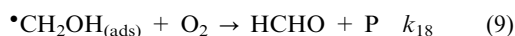
The reaction with O_2 can explain why only a small part of the adsorbate species can be detected by this technique when methanol is present in the solution. Indeed the reaction described by eqn (9) is fast in homogeneous aqueous solution ($k = 5 \times 10^9$ M^{-1} s^{-1}).

Conclusions

We have demonstrated that the surface interrogation mode of SECM, SI-SECM, is useful in characterizing photo-electrochemical reactions on semiconductors by the detection, quantification and evaluation of decay kinetics of the photo-generated adsorbed hydroxyl radical $^\bullet OH_{(ads)}$ on a nanostructured TiO_2 electrode. The mediator pair $IrCl_6^{2-/3-}$ was a suitable interrogation agent, resistant to the strongly oxidizing conditions found in the photoelectrochemical setup and unreactive with products of the $^\bullet OH_{(ads)}$ generation process (*e.g.* H_2O_2 and O_2). This mediator can also be generated on a Au UME at a potential where the electrode does not collect interfering species. Furthermore, its reaction with $^\bullet OH_{(ads)}$ is fast enough to allow quantitative evaluation of the rate constant ($k_{SI} = 3$ m^3 mol^{-1} s^{-1}). The mediator response fits conventional SECM feedback theory showing positive feedback at the illuminated TiO_2 surface, and negative feedback under dark conditions. In SI-SECM experiments in the dark, the reduced form of the mediator can react chemically with $^\bullet OH_{(ads)}$ to produce a transient feedback making possible quantification of the decay kinetics of the adsorbate. A maximum surface coverage for our TiO_2 electrodes was $\Gamma_{\text{max}} = 3.5 \times 10^{-5}$ mol m^{-2} or $Q_{\text{max}} = 338$ μC cm^{-2}, which is at least an order of magnitude smaller than the area determined by dye adsorption experiments. We also found the rate constant for the second order decay process of $^\bullet OH_{(ads)}$ dimerization to H_2O_2 to be $k_{OH} = 2.2 \times 10^3$ mol^{-1} m^2 s^{-1}. Scavenger experiments in which 2 M methanol was added to the solution to react with $^\bullet OH_{(ads)}$ yielded a pseudo-first order reaction constant of $k'_{\text{MeOH}} = 1$ s^{-1}; this reaction also produced an adsorbed species that also reacted with the tip-generated $IrCl_6^{3-}$ as well. This SI-SECM technique, inherently an *in situ* method, has been proven useful then for the extraction of quantitative information from the formation and decay of adsorbed species at a representative photocatalyst. Since its application does not depend on the spectroscopic characteristics of the adsorbate at the substrate nor its voltammetric behavior, the technique should be useful for the study of different photocatalytic surfaces, *e.g.* well-defined single crystals.

Acknowledgements

References

1 A. Fujishima and K. Honda, *Nature*, 1972, **238**, 37.
2 S. U. M. Khan, M. Al-Shahry and W. B. Ingler, *Science*, 2002, **297**, 2243.
3 G. K. Mor, K. Shankar, M. Paulose, O. K. Varghese and C. A. Grimes, *Nano Lett.*, 2005, **5**, 191.
4 G. N. Schrauzer and T. D. Guth, *J. Am. Chem. Soc.*, 1977, **99**, 7189.
5 A. Piscopo, D. Rober and J. V. Weber, *J. Photochem. Photobiol., A*, 2001, **139**, 253.

6 A. Mills, R. H. Davies and D. Worsley, *Chem. Soc. Rev.*, 1993, **22**, 417.

7 D. Chatterjee and S. Dasgupta, *J. Photochem. Photobiol., C*, 2005, **6**, 186.

8 J. M. Herrmann, J. Disdier, P. Pichat, S. Malato and J. Blanco, *Appl. Catal., B*, 1998, **17**, 15.

9 L.-M. Liu, P. Crawford and P. Hu, *Prog. Surf. Sci.*, 2009, **84**, 155.

10 R. Wang, N. Sakai, A. Fujishima, T. Watanabe and K. Hashimio, *J. Phys. Chem. B*, 1999, **103**, 2188.

11 J. G. Yu, X. J. Zhao and Q. N. Zhao, *Thin Solid Films*, 2000, **379**, 7.

12 L.-Q. Wang, D. R. Baer, M. H. Engelhard and A. N. Shultz, *Surf. Sci.*, 1995, **344**, 237.

13 *Scanning Electrochemical Microscopy*, ed. A. J. Bard and M. V. Mirkin, Marcel Dekker, New York, 2001, ch. 6.

14 J. Rodríguez-López, M. A. Alpuche-Aviles and A. J. Bard, *J. Am. Chem. Soc.*, 2008, **130**, 16985.

15 T. Hirakawa and Y. Nosaka, *Langmuir*, 2002, **18**, 3247.

16 D. Lawless, N. Serpone and D. Meisel, *J. Phys. Chem.*, 1991, **95**, 5166.

17 C. B. Almquist and P. Biswas, *J. Catal.*, 2002, **212**, 145.

18 S. Kim and W. Choi, *Environ. Sci. Technol.*, 2002, **36**, 2019.

19 N. Sakai, A. Fujishima, T. Watanabe and K. Hashimoto, *J. Phys. Chem. B*, 2003, **107**, 1028.

20 P. M. Kumar, S. Badrinarayanan and M. Sastry, *Thin Solid Films*, 2000, **358**, 122.

21 H. Jensen, A. Soloviev, Z. S. Li and E. G. Sogaard, *Appl. Surf. Sci.*, 2005, **246**, 239.

22 C. D. Jaeger and A. J. Bard, *J. Phys. Chem.*, 1979, **83**, 3146.

23 G. Riegel and J. R. Bolton, *J. Phys. Chem.*, 1995, **99**, 4215.

24 M. A. Grela, M. E. J. Coronel and A. J. Colussi, *J. Phys. Chem.*, 1996, **100**, 16940.

25 D. Mandler and A. J. Bard, *J. Electrochem. Soc.*, 1990, **137**, 2468.

26 S. K. Haram and A. J. Bard, *J. Phys. Chem. B*, 2001, **105**, 8192.

27 J. Rodríguez-López, A. Minguzzi and A. J. Bard, *J. Phys. Chem. C*, 2010, **114**, 18645.

28 J. Rodríguez-López and A. J. Bard, *J. Am. Chem. Soc.*, 2010, **132**, 5121.

29 Q. Wang, J. Rodríguez-López and A. J. Bard, *J. Am. Chem. Soc.*, 2009, **131**, 17046.

30 D. O. Wipf and A. J. Bard, *J. Electrochem. Soc.*, 1991, **138**, 469.

31 H. Xiong, J. Guo and S. Amemiya, *Anal. Chem.*, 2007, **79**, 2735.

32 J. Rodríguez-López, M. A. Alpuche-Aviles and A. J. Bard, *Anal. Chem.*, 2008, **80**, 1813.

33 C. A. Nijhuis, J. K. Sinha, G. Wittstock, J. Huskens, B. J. Ravoo and D. N. Reinhoudt, *Langmuir*, 2006, **22**, 9770.

34 M. J. W. Ludden, J. K. Sinha, G. Wittstock, D. N. Reinhoudt and J. Huskens, *Org. Biomol. Chem.*, 2008, **6**, 1553.

35 K. Shankar, J. I. Basham, N. K. Allam, O. K. Varghese, G. K. Mor, X. Feng, M. Paulose, J. A. Seabold, K.-S. Choi and C. A. Grimes, *J. Phys. Chem. C*, 2009, **113**, 6327.

36 H. A. Schwarz and R. W. Dodson, *J. Phys. Chem.*, 1984, **88**, 3643.

37 C. M. Sánchez-Sánchez, J. Rodríguez-López and A. J. Bard, *Anal. Chem.*, 2008, **80**, 3254.

38 J. Zhang, C. J. Slevin, C. Morton, P. Scott, D. J. Walton and P. R. Unwin, *J. Phys. Chem. B*, 2001, **105**, 11120.

39 C. J. Slevin and P. R. Unwin, *J. Am. Chem. Soc.*, 2000, **122**, 2597.

40 P. R. Unwin and A. J. Bard, *J. Phys. Chem.*, 1992, **96**, 5035.

41 J. Marugán, D. Hufschmidt, M.-J. López-Muñoz, V. Selzer and D. Bahnemann, *Appl. Catal., B*, 2006, **62**, 201.

42 J. Marugán, D. Hufschmidt, M.-J. López-Muñoz, V. Selzer and D. Bahnemann, *Appl. Catal., B*, 2006, **62**, 201.

43 C.-Y. Wang, J. Rabani, D. W. Bahnemann and J. K. Dohrman, *J. Photochem. Photobiol., A*, 2002, **148**, 169.

44 Y. Du and J. Rabani, *J. Phys. Chem. B*, 2003, **107**, 11970.